Distributed Localization of a RF target in NLOS Environments

Wenjie Xu, François Quitin, *Member, IEEE*, Mei Leng, *Member, IEEE*,
Wee Peng Tay, *Senior Member, IEEE*, and Sirajudeen G. Razul

Abstract

We propose a novel distributed expectation maximization (EM) method for non-cooperative RF target localization using a wireless sensor network. We consider the scenario where few or no sensors receive line-of-sight signals from the target. In the case of non-line-of-sight signals, the signal path consists of a single reflection between the transmitter and receiver. Each sensor is able to measure the time difference of arrival of the target's signal with respect to a reference sensor, as well as the angle of arrival of the target's signal. We derive a distributed EM algorithm where each node makes use of its local information to compute summary statistics, and then shares these statistics with its neighbors to improve its estimate of the target localization. We show that our distributed algorithm converges, and simulation results suggest that our method achieves an accuracy close to the centralized EM algorithm. We apply the distributed EM algorithm to a set of experimental measurements with a network of four nodes, which confirm that the algorithm is able to localize a RF target in a realistic non-line-of-sight scenario.

Index Terms

Target localization, expectation maximization, distributed algorithm, wireless sensor network

I. INTRODUCTION

A wireless sensor network (WSN) consists of a large number of distributed devices that have limited sensing, communication and processing capabilities. RF target localization is an important

application of WSNs in which multiple sensors collect and cooperatively process the location information gathered from the wireless signal transmitted by the target. There are many fields in which WSN localization is used. One example is the accurate localization of mobile phones in search and rescue operations, which has the potential to significantly reduce emergency response time. Another example is tracking of wildlife in large areas, which can be challenging because of the large areas to be monitored. A more commercial application is the localization and tracking of customers in a shopping area, or the precise localization of social network users in urban environment. The latter can be challenging because the line-of-sight between the RF target and sensors is often obstructed in cluttered urban environments.

When the target is cooperative, the target can include a timestamp in its transmitted message indicating when the message was transmitted. It is then possible to use time-of-arrival (TOA) techniques to localize the target, provided the target and the sensors can be synchronized. However, in the case of non-cooperative RF targets, one must resort to time-difference-of-arrival (TDOA) or angle-of-arrival (AOA) techniques. These techniques have been widely investigated in the context of line-of-sight (LOS) scenarios, where a LOS exist between the target and the different sensing nodes. In practical cases, however, it is rare to have LOS signals, especially in urban environments. Another problem is that traditional localization algorithms are centralized, and they require all sensor data to be transmitted to a fusion sensor. In practice, sensors are often randomly scattered in the environment, and each sensor has limited energy storage. If a random sensor is selected to be the fusion sensor, it may quickly deplete its energy reserve due to the high processing costs involved. Such a network is also vulnerable to the failure of the fusion sensor. Distributed algorithms, on the other hand, have drawn a lot of attention due to the fact that they can distribute the processing load among sensors by leveraging local data transmission and local processing. In this work, we investigate the target localization problem when we have predominantly non-line-of-sight (NLOS) signals. We model the NLOS signals using a single-bounce path between target and sensor, without knowing the location of the scatterer. As the target is non-cooperating, we consider that only TDOA and AOA information is available at the sensors, and we investigate the use of distributed algorithms to perform the target localization.

A. Main Contributions

The contributions of this paper can be summarized as follows:

- We propose a distributed generalized expectation maximization (EM) algorithm for non-cooperative RF target localization in NLOS environments. The distributed EM algorithm utilizes TDOA and AOA information at each sensor node, and treats the orientations of the scatterers from which signals are bounced off as unobserved latent variables. The locations of the scatterers are assumed to be unknown. We provide a proof to show that, under some sufficient conditions, the proposed distributed algorithm converges to a local optimum of the likelihood function.

- We provide simulation results to show the performance of the distributed EM algorithm, and compare it with a centralized EM algorithm that serves as a benchmark. We analyze the performances of the results for different TDOA and AOA noise values.

- We perform an experimental measurement campaign and apply the distributed EM algorithm on a set of experimental results in which we have 1 LOS and 3 NLOS nodes to the target. Our results show that the distributed EM algorithm performs well when applied on this realistic scenario, and achieves localization accuracies below 15 m for 90% of the measurements, where the TDOA measurements are up to 160 m.

B. Related Works

Localization techniques based on wireless TDOA have been extensively investigated, ranging from a few decades back [1]–[3] to the present [4]–[8]. Approaches robust to NLOS errors have been proposed in [9], [10]. These approaches assume that a sufficient number of sensors receive the LOS signals, and NLOS errors are filtered out by making use of either LOS measurements or a predicted target position. In [11], [12], NLOS errors are modeled as positive biases and their statistical characteristics are learned by methods such as bootstrap sampling [11] and particle filters [12]. These techniques however require a large number of observations, and are computationally expensive. Also of interest is [13] where the measured MIMO signal is compared with a ray-tracing-generated database to determine the transmitter's location. However, the latter requires to have a precise map of the environment, which might be impractical in many applications. In [14], the authors use TOA and propose to estimate the measurement probability density function (pdf) through an iterative process. Once the measurement pdf is known, one is able to retrieve the target location. In [15], the TOA is modeled as a two-mode mixture distribution (even though the underlying process may be different) whose parameters are estimated through different techniques. Both works assume that the TOA measurement

pdf remains static for a given environment, which might prove to be a somewhat unrealistic assumption in practical scenarios.

To avoid estimating the pdf of NLOS errors, we consider a ray-tracing approach that uses the TOA of a single bounce path between the target and sensor, as well as the corresponding AOA and angle-of-departure (AOD) [16]–[18]. However, since we assume that our target is non-cooperative, sensors have no access to the AOD information. Furthermore, we do not assume that sensors have knowledge of the target signal structure, so only TDOA and AOA information are available at the sensors. In this formulation, the orientation angles of the scatterers are treated as latent variables, therefore we appeal to the EM algorithm [19] to estimate the target position. A distributed EM algorithm where a message has to cycle across the entire network through a predefined sensor sequence has been proposed in [20], which makes it susceptible to sensor failures. Another distributed EM algorithm has been recently proposed in [21], [22], where the local likelihoods at each sensor belong to the exponential family. The system model in our problem unfortunately does not belong to this class of distributions, and we have to develop a new distributed EM algorithm based on [23] for target localization in NLOS environments. The EM algorithm uses an alternating maximization at the M-step performed at each sensor. We show that under certain technical conditions, our distributed EM algorithm allows the target position estimates at all sensors to converge to the same estimate, which is a local maximizer of the likelihood function.

The rest of this paper is organized as follows. In Section II, we present our system model. We briefly review the centralized EM method for target localization, and then propose a distributed EM algorithm in Section III. In Section IV, we provide a convergence analysis for our distributed EM algorithm, and we verify its performance through simulations in Section V. We evaluate the performance of our distributed EM algorithm in a real scenario by using measurements collected with our USRP-software defined radio platrform in Section VI. Finally, we conclude in Section VII.

Notations: Let $\mathbb{R}$ be the real space, and for any vector $y \in \mathbb{R}^d$, let $\|y\|$ be its Euclidean norm. For any $\mathcal{E} \subset \mathbb{R}^m$, let $d(x, \mathcal{E}) = \inf\{\|x - y\| : y \in \mathcal{E}\}$. For any vectors $y_1, \ldots, y_N$ in $\mathbb{R}^d$, the concatenated vector $[y_1^T, \ldots, y_N^T]^T$ is denoted as $\mathbf{y} = \text{Vec}(\{y_i\}_{i=1}^N)$. We also use $\text{Vec}(A)$ to denote the vector formed by stacking the columns of the matrix A together. We let $\langle \mathbf{y} \rangle \triangleq (y_1 + \ldots + y_N)/N \in \mathbb{R}^d$, be the average vector of $y_1, \ldots, y_N$. We denote by $\mathbf{y}_\perp \triangleq \mathbf{y} - \mathbf{1} \otimes \langle \mathbf{y} \rangle$ the disagreement vector, where $\mathbf{1}$ is the vector containing all ones, and $\otimes$ is the Kronecker

product. We use $\langle \cdot, \cdot \rangle$ to denote inner product, $\nabla_x f(x)$ to be the gradient with respect to (w.r.t.) x of the function f, and I_d to denote the $d \times d$ identity matrix.

II. SYSTEM MODEL

We consider a network of N nodes, where each node has either one single-bounce NLOS signal path or a LOS signal path to the target, as shown in Figure 1. The target could for example be a cell phone user to be localized and tracked, and the sensor nodes diverse picocell base stations deployed in the surrounding area. Let d_i be the length of the signal path from the
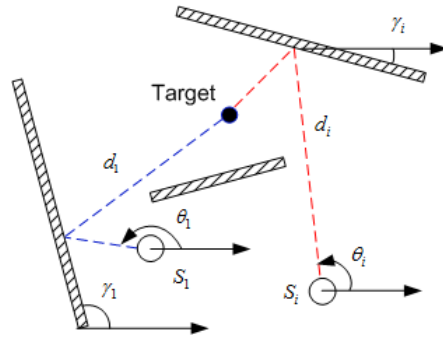

Fig. 1. An example for the one-bounce reflection path from the target to sensor i and sensor 1.

target to node i, θ_i be the AOA of the signal path at node i, and γ_i be the orientation of the scatterer from which the signal path from the target to node i bounces off. If the signal path is a LOS path, we take the scatterer orientation to be the same as the AOA θ_i. All angles are measured with respect to the horizontal direction. It can be shown [24] that

$$d_i = \mathbf{g}(\theta_i, \gamma_i)^T (\mathbf{q} - \mathbf{p}_i)$$

where $\mathbf{q}$ is the target location, $\mathbf{p}_i$ denotes the position of the i-th node and $\mathbf{g}(\theta_i, \gamma_i)$ is defined as

$$\mathbf{g}(\theta_i, \gamma_i) \triangleq \frac{1}{\cos(\theta_i - \gamma_i)} \begin{bmatrix} \cos \gamma_i \\ \sin \gamma_i \end{bmatrix}.$$

Without loss of generality, sensor 1 is selected as the reference node, and every other sensor $i \geq 2$ computes a TDOA measurement w.r.t. to node 1 given by

$$\tilde{d}_{i1} = \mathbf{g}(\theta_i, \gamma_i)^T (\mathbf{q} - \mathbf{p}_i) - \mathbf{g}(\theta_1, \gamma_1)^T (\mathbf{q} - \mathbf{p}_1) + \tilde{n}_i, \tag{1}$$

where $\tilde{n}_i$ is the TDOA measurement noise at node i. The measurement noises are assumed to be independent zero-mean Gaussian random variables with $\tilde{n}_i$ having variance σ_i^2 for all $i = 1, \ldots, N$. In addition, each node $i \geq 2$ makes a noisy AOA measurement $\tilde{\theta}_i$, modeled by $\tilde{\theta}_i = \theta_i + \eta_i$ where η_i is the AOA measurement noise, which is assumed to be independent of the TDOA measurement noise and across nodes. We further assume that the AOA noise η_i follows a uniform distribution, i.e., $\mathrm{Unif}[-\eta^0, \eta^0]$.

The orientation angles γ_i, for $i \geq 2$, are treated as latent variables that are not observed with $\gamma_i \in \Gamma_i = \{\beta_1, \cdots, \beta_M\}$, where $\beta_j \in [0, 2\pi)$ for $j = 1, \ldots, M$. If the reflector angles γ_i can be estimated, the support set Γ_i can be limited to a few discrete values around the estimated angle γ_i^0. If the reflector orientation is completely unknown, the geometry of the environment can be used to limit the support set Γ_i, e.g. in the case of a street with rectangular buildings, the support set can be limited to $\Gamma_i = \{0°, 45°, 90°, 135°, 180°\}$. The effect of different scatterer orientation support set will be investigated in more detail in Section VI-B. The reflector orientation γ_1 of the signal received at sensor 1, is assumed to be known (uncertainty in the value of γ_1 can be included in the noise term on the right hand side of (1)), because otherwise the estimation problem becomes unidentifiable due to the existence of multiple global maximum points in the likelihood function (see Figure 2 for an example). This can be achieved in practice by having sensor 1 estimate the reflector angles in its surroundings using methods in [25], [26]. Another possibility is to combine the AOA of sensor 1 with knowledge of the surroundings of this sensor to estimate the angle γ_1.
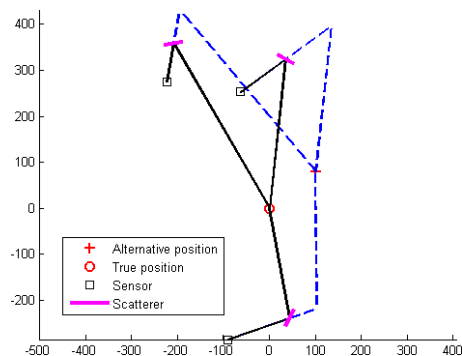

Fig. 2. An example in which a set of TDOA and AOA measurements correspond to two possible target locations if no additional information about the scatterers are known. Because any constant added to all the signal path lengths do not change the TDOA values, it is possible to find multiple target locations that satisfy the same AOA measurements.

Symbol	Definition
θ_i	AOA at node i
γ_i	Scatterer angle for node i
d_i	Signal path length between target and node i
$\mathbf{q}$	location of target
$\mathbf{p}_i$	location of node i
$\tilde{d}_{i1}$	TDOA measurement between node i and node 1
$\mathbf{x}_i^n$	parameter vector containing $\mathbf{q}$ and $\{\theta_i\}_{i=1}^N$ at node i at iteration n
z_i	$z_i = \{\tilde{d}_{i1}, \theta_i, \gamma_i\}$, contains estimates of TDOA, AOA and scatterer angles of node i
$\rho_i(\gamma_i, \mathbf{x}^{n-1})$	conditional probability of the scatterer angle at node i, refer to (4)
$S_i(z_i; \theta_1), T_i(z_i; \mathbf{q})$	local statistics at node i (before E-step), refer to (5)-(6)
s_i^n, t_i^n	local statistics at node i (after E-step) at iteration n, refer to (9)-(10)
λ_n	step size at iteration n
ϕ_1, ϕ_2	local maximizer functions of $\mathbf{q}$ and θ_1, refer to (5)-(6)
$K(\mathbf{x})$	log-likelihood function after E-step, refer to (14)

It should be noted that some of the above assumptions may not always be true. For example, the TDOA noise might be correlated, and might not have a Gaussian distribution. However, in order to derive a *provably convergent* target localization algorithm, the above assumptions are necessary. Considering more complicated distributions will lead to an unsolvable problem for target localization. However, we will show in Section VI that our algorithms still perform well when applied to measured data, where all the above assumptions might not necessarily hold.

For the convenience of the reader, we summarize some of the notations we use throughout this paper in Table I. Several of the notations in Table I will be defined formally where they first appear in the paper.

III. EM ALGORITHMS FOR TARGET LOCALIZATION

In this section, we start by providing a brief review of the standard centralized EM method for target localization, and then describe our distributed EM method. It should be noted that for centralized algorithms, the fusion sensor has access to all TDOA and AOA measurements, whereas in the distributed algorithm each sensor has only access to its own measurements and the information from sensor 1. The distributed algorithm aims to emulate the performance of the centralized algorithm by using only the local information at each sensor.

A. Centralized EM algorithm

In the centralized EM method we want to estimate the target location $\mathbf{q}$, where the reflector orientations $\{\gamma_i\}_{i=2}^N$ are taken to be missing data. Let $\mathbf{x} = [\mathbf{q}^T, \{\theta_i\}_{i=1}^N]^T$ be the parameters of interest. Then, the log likelihood function for the complete data is given by $\log p\left(\{\tilde{d}_{i1}, \tilde{\theta}_i, \gamma_i\}_{i=2}^N, \tilde{\theta}_1 \middle| \mathbf{x}\right)$.

Each angle γ_i is confined to a support set $\Gamma_i = \{\beta_1, \ldots, \beta_M\}$, and is independent of the other reflector angles. Let ψ_i be the angle of $\mathbf{q} - \mathbf{p}_i$ w.r.t. the horizontal direction. A vector with orientation angle $\phi_i = 2\gamma_i - \theta_i$ w.r.t. the horizontal has opposite direction to the vector from the target to the scattering point. It is shown in Appendix A that the space of possible source locations is restricted to the area spanned by the line from node i in the direction of the AOA and the line from node i in the direction opposite to the AOD, as shown in Figure 3. Since we assume that we do not have a priori knowledge of the reflector orientations for sensor $i \geq 2$, we assume

$$p\left(\gamma_i \middle| \mathbf{q}, \theta_i\right) \propto \begin{cases} 1 & \text{if } \psi_i \in [\min(\phi_i, \theta_i), \max(\phi_i, \theta_i)], \\ 0 & \text{otherwise} . \end{cases}$$
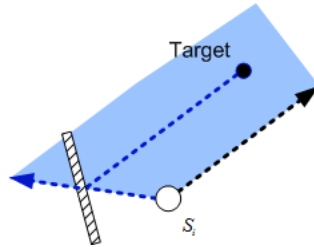

Fig. 3. The source lies in the area spanned by the line from node i in the direction of AOA and the line from node i in the direction opposite to the AOD.

From our model assumptions, given θ_i, $\tilde{\theta}_i$ is independent of the other random variables in the complete data, and since TDOA measurements and scatterer orientations are independent across

sensors $i \geq 2$, we have

$$\log p\left(\{\tilde{d}_{i1}, \tilde{\theta}_i, \gamma_i\}_{i=2}^N, \tilde{\theta}_1 \Big| \mathbf{x}\right)$$

$$= \sum_{i=1}^N \log p(\tilde{\theta}_i | \theta_i) + \sum_{i=2}^N \log p\left(\gamma_i, \tilde{d}_{i1} \Big| \mathbf{x}\right)$$

$$= \sum_{i=1}^N \log p(\tilde{\theta}_i | \theta_i) + \sum_{i=2}^N \log p\left(\gamma_i | \mathbf{q}, \theta_i\right)$$

$$+ \sum_{i=2}^N \log p\left(\tilde{d}_{i1} \Big| \mathbf{q}, \theta_i, \theta_1, \gamma_i\right), \tag{2}$$

where the last equality follows from (1). Since the TDOA measurement error is Gaussian, we obtain

$$p\left(\tilde{d}_{i1} \Big| \mathbf{q}, \theta_i, \theta_1, \gamma_i\right) =$$

$$\frac{1}{\sqrt{2\pi\sigma_i^2}} \exp\left(-\frac{1}{2\sigma_i^2}(\tilde{d}_{i1} + g(\theta_i, \gamma_i)^T \mathbf{p}_i - g(\theta_1, \gamma_1)^T \mathbf{p}_1 - (g(\theta_i, \gamma_i) - g(\theta_1, \gamma_1))^T \mathbf{q})^2\right).$$

The EM algorithm is an iterative procedure where a new estimate $\mathbf{x}^n$ is generated at each iteration n. The estimation is done by repeating the following two steps, where $\mathbf{x}^0$ is an initial guess.

1) *E-step.* The E-step is to account for the missing data, in this case the scatterer orientation angle. At iteration n, we have

$$Q\left(\mathbf{x} | \mathbf{x}^{n-1}\right) = \int_{\{\gamma_i\}_{i=2}^N} \log p\left(\{\tilde{d}_{i1}, \tilde{\theta}_i, \gamma_i\}_{i=2}^N, \tilde{\theta}_1 \Big| \mathbf{x}\right)$$

$$\cdot p\left(\{\gamma_i\}_{i=2}^N \Big| \mathbf{x}^{n-1}, \{\tilde{d}_{i1}, \tilde{\theta}_i\}_{i=2}^N, \tilde{\theta}_1\right) \mathrm{d}\gamma_2 \dots \gamma_N \tag{3}$$

Since conditioned on $(\tilde{d}_{i1}, \mathbf{q}^{n-1}, \theta_i^{n-1}, \theta_1^{n-1})$, γ_i is independent across sensors and of $\tilde{\theta}_i$, we can write

$$p\left(\{\gamma_i\}_{i=2}^N \Big| \mathbf{x}^{n-1}, \{\tilde{d}_{i1}, \tilde{\theta}_i\}_{i=2}^N, \tilde{\theta}_1\right)$$

$$= \prod_{i=2}^N p\left(\gamma_i | \tilde{d}_{i1}, \mathbf{q}^{n-1}, \theta_i^{n-1}, \theta_1^{n-1}\right).$$

Let us define

$$\rho_i(\gamma_i, \mathbf{x}^{n-1}) \triangleq p\left(\gamma_i | \tilde{d}_{i1}, \mathbf{q}^{n-1}, \theta_i^{n-1}, \theta_1^{n-1}\right)$$

$$\propto p\left(\tilde{d}_{i1} \Big| \mathbf{q}^{n-1}, \theta_i^{n-1}, \theta_1^{n-1}, \gamma_i\right) p\left(\gamma_i | \mathbf{q}^{n-1}, \theta_i^{n-1}, \theta_1^{n-1}\right), \tag{4}$$

which follows from Bayes' theorem. By substituting (2) in (3) (and noticing that $\log p(\tilde{\theta}_i|\theta_i)$ does not depend on $\{\gamma_i\}_{i=2}^N$), (3) can be rewritten as

$$Q\left(\mathbf{x}|\mathbf{x}^{n-1}\right) = \sum_{i=1}^{N} \log p(\tilde{\theta}_i|\theta_i)$$

$$+ \sum_{i=2}^{N} \int_{\gamma_i} \log p\left(\gamma_i|\mathbf{q}, \theta_i\right) \rho_i(\gamma_i, \mathbf{x}^{n-1}) \mathrm{d}\gamma_i$$

$$+ \sum_{i=2}^{N} \int_{\gamma_i} \log p\left(\tilde{d}_{i1}\Big|\mathbf{q}, \theta_i, \theta_1, \gamma_i\right) \rho_i(\gamma_i, \mathbf{x}^{n-1}) \mathrm{d}\gamma_i.$$

2) *M-step*. A new estimate of $\mathbf{x}^n$ is obtained by maximizing the function $Q(\mathbf{x}, \mathbf{x}^{n-1})$, i.e.,

$$\mathbf{x}^n = \arg\max_{\mathbf{x}} Q\left(\mathbf{x}|\mathbf{x}^{n-1}\right).$$

The EM algorithm is not guaranteed to converge to the optimal solution, as it can get stuck in a local maximum [27], [28]. In practice, one can initialize the EM algorithm at different values for $\mathbf{x}^0$, and if the different runs yield different solutions, select the result with the highest log-likelihood value.

B. Distributed EM algorithm

We now propose a distributed EM algorithm based on the algorithm described in Section III-A, and the distributed EM algorithm of [21], [22], which require that the local likelihood functions in (2) belong to the exponential family. We note that our local likelihood functions do not belong to the exponential family of distributions if both the target location $\mathbf{q}$ and AOA θ_1 are parameters to be estimated. To overcome this difficulty, we write the local likelihood function in two different ways: each time keeping either $\mathbf{q}$ or θ_1 (but not both) as the single parameter of interest. By performing this decomposition, and a sequential optimization in the M-step, it turns out that the procedure of [21], [22] can be adapted to perform distributed estimation of our target location. However, the convergence of our proposed method does not follow directly from the analysis in [21], [22], and we require further technical assumptions and convergence analysis, although similar conclusions as in [21], [22] are derived.

We assume that each sensor i knows its own location $\mathbf{p}_i$ and sensor 1 broadcasts its information $(\mathbf{p}_1, \gamma_1, \tilde{\theta}_1)$ to all sensors. In the following, we show that the first two terms in the complete data likelihood given by (2) can be converted to constraints on $\{\theta_i\}_{i=1}^N$ and $\mathbf{q}$.

Since the TDOA measurement noise is Gaussian, the local log-likelihood function of node i is given by

$$\log p\left(\tilde{d}_{i1} \middle| \mathbf{q}, \theta_1, \theta_i, \gamma_i\right)$$

$$= -\frac{1}{2\sigma_i^2}\left(\tilde{d}_{i1} - \mathbf{g}(\theta_i, \gamma_i)^T(\mathbf{q} - \mathbf{p}_i) + \mathbf{g}(\theta_1, \gamma_1)^T(\mathbf{q} - \mathbf{p}_1)\right)^2$$

We now rewrite the local log-likelihood functions in different ways, so as to isolate terms that depend on $\mathbf{q}$ or θ_1 only. After some algebraic manipulations (which are omitted here), and by defining $z_i = \{\tilde{d}_{i1}, \theta_i, \gamma_i\}$, the local log-likelihood can be written as

$$\log p\left(\tilde{d}_{i1} \middle| \mathbf{q}, \theta_1, \theta_i, \gamma_i\right)$$

$$= c_{1,i}(z_i, \theta_1) + S_i(z_i; \theta_1)^T \phi_1(\mathbf{q}) \tag{5}$$

$$= c_{2,i}(z_i, \mathbf{q}) + T_i(z_i; \mathbf{q})^T \phi_2(\theta_1) \tag{6}$$

$$\triangleq \psi_i(z_i, \mathbf{q}, \theta_i, \theta_1) \tag{7}$$

where $c_{1,i}(\cdot)$ and $c_{2,i}(\cdot)$ are normalizing factors, $\phi_2(\theta_1) = [1/\cos^2(\theta_1 - \gamma_1), 1/\cos(\theta_1 - \gamma_1)]^T$, and

$$\phi_1(\mathbf{q}) = \begin{bmatrix} \mathrm{Vec}(\mathbf{q}\mathbf{q}^T) \\ \mathbf{q} \end{bmatrix}, \quad S_i(z_i; \theta_1) = \begin{bmatrix} \mathrm{Vec}(\mathbf{U}_i) \\ -2\mathbf{V}_i \end{bmatrix} \tag{8}$$

with

$$\mathbf{U}_i = -\frac{1}{2\sigma_i^2}(\mathbf{g}(\theta_i, \gamma_i) - \mathbf{g}(\theta_1, \gamma_1))(\mathbf{g}(\theta_i, \gamma_i) - \mathbf{g}(\theta_1, \gamma_1))^T,$$

$$\mathbf{V}_i = -\frac{1}{2\sigma_i^2}(\tilde{d}_{i1} + \mathbf{g}(\theta_i, \gamma_i)^T\mathbf{p}_i - \mathbf{g}(\theta_1, \gamma_1)^T\mathbf{p}_1)$$

$$\cdot (\mathbf{g}(\theta_i, \gamma_i) - \mathbf{g}(\theta_1, \gamma_1)),$$

and

$$T_i(z_i; \mathbf{q}) = -\frac{1}{2\sigma_i^2}$$

$$\cdot \begin{bmatrix} \left(\begin{bmatrix} \cos\gamma_1 \\ \sin\gamma_1 \end{bmatrix}^T (\mathbf{q} - \mathbf{p}_1)\right)^2 \\ 2(\tilde{d}_{i1} - \mathbf{g}(\theta_i, \gamma_i)^T(\mathbf{q} - \mathbf{p}_i)) \begin{bmatrix} \cos\gamma_1 \\ \sin\gamma_1 \end{bmatrix}^T (\mathbf{q} - \mathbf{p}_1) \end{bmatrix}.$$

Note that if θ_1 is known, (5) belongs to the exponential family. Similarly, if $\mathbf{q}$ is known, (6) belongs to the exponential family.

The fundamental idea of our distributed EM algorithm is to adapt the local log-likelihood functions (5)-(6) of the different nodes so that they approximate the complete log-likelihood function in (2). During each iteration of the distributed EM algorithm, the nodes perform the following three steps: the nodes first perform a local E-step to account for the missing scatterer orientation data. This is followed by a gossip step in which nodes exchange appropriate statistics with their neighbors so that their local log-likelihood functions approximate the complete log-likelihood function. Finally, each node performs a local M-step to determine the parameters $\mathbf{x} = [\mathbf{q}^T, \{\theta_i\}_{i=1}^N]^T$ that maximize its log-likelihood function. Under the technical conditions given in Assumptions 1, 2 and 3 below, the estimates of all the nodes converge to an identical solution. In the following, we let $\mathbf{x}_i^n = [(\mathbf{q}_i^n)^T, \theta_{1,i}^n, \theta_i^n]^T$ be the local estimate at node i of the parameters $[\mathbf{q}^T, \theta_1, \theta_i]$ at iteration n. The distributed EM algorithm is given as follows:

1) *Local E-step:* At each iteration, each sensor accounts for its missing data (i.e., the scatterer orientation):

$$\bar{s}_i(\mathbf{x}) = \int_{\gamma_i} S_i(z_i; \theta_1)\rho_i(\gamma_i, \mathbf{x})\mathrm{d}\gamma_i,$$

$$\bar{t}_i(\mathbf{x}) = \int_{\gamma_i} T_i(z_i; \mathbf{q})\rho_i(\gamma_i, \mathbf{x})\mathrm{d}\gamma_i,$$

$$\bar{\psi}_i(\theta_i, \mathbf{q}, \theta_1; \mathbf{x}) = \int_{\gamma_i} \psi_i(z_i, \mathbf{q}, \theta_i, \theta_1)\rho_i(\gamma_i, \mathbf{x})\mathrm{d}\gamma_i.$$

Each node i then computes the local statistics $\tilde{s}_i^n$ and $\tilde{t}_i^n$:

$$\tilde{s}_i^n = s_i^{n-1} + \lambda_n[\bar{s}_i(\mathbf{x}_i^{n-1}) - s_i^{n-1}], \tag{9a}$$

$$\tilde{t}_i^n = t_i^{n-1} + \lambda_n[\bar{t}_i(\mathbf{x}_i^{n-1}) - t_i^{n-1}], \tag{9b}$$

where $\lambda_n \geq 0$ is a chosen step size. This update process is to ensure that information from the other nodes obtained in previous iterations (contained in s_i^{n-1} and t_i^{n-1}) is maintained during the current iteration.

2) *Gossip step:* Each node i broadcasts $\{\tilde{s}_i^n, \tilde{t}_i^n\}$ to its neighbors, and collects $\{\tilde{s}_j^n, \tilde{t}_j^n\}$ from its neighboring sensors j. It then computes the weighted average:

$$s_i^n = \sum_{j=2}^{N} w_n(i,j) \tilde{s}_j^n \tag{10a}$$

$$t_i^n = \sum_{j=2}^{N} w_n(i,j) \tilde{t}_j^n \tag{10b}$$

where $w_n(i,j)$ are non-negative weights, with $w_n(i,j) = 0$ if node j is not a neighbor of node i. This step enables node i to approximate the the log-likelihood function in the last term in (2) (note that the first two terms in (2) have been converted to constraints on $\{\theta_i\}_{i=1}^{N}$ and $\mathbf{q}$).

3) *Local M-step:* Each node determines the value of $\mathbf{x}_i^n$ that maximizes its local log-likelihood function as follows:

$$\mathbf{q}_i^n = \max_{\mathbf{q} \in A_i} (s_i^n)^T \phi_1(\mathbf{q}), \tag{11}$$

$$\theta_{1,i}^n = \max_{\theta_1 \in \Theta_1} (t_i^n)^T \phi_2(\theta_1), \tag{12}$$

$$\theta_i^n = \max_{\theta_i \in \Theta_i} \bar{\psi}_i(\theta_i, \mathbf{q}_i^n, \theta_{1,i}^n; \mathbf{x}_i^{n-1}), \tag{13}$$

where $A_i = \{\mathbf{q} : p(\mathbf{q}|\gamma, \theta_i) > 0 \text{ for } \gamma \in \Gamma\}$ and $\Theta_i = [\tilde{\theta}_i - \eta^0, \tilde{\theta}_i + \eta^0]$ are the constraint sets corresponding to the first two terms of (2). Optimizing separately over each parameter $\mathbf{q}$, θ_1 and θ_i is much easier than performing a joint maximization over all three parameters, as each optimization in (11)-(13) has a unique global maximum. We will see in Theorem 1 that this also ensures that the estimated $\mathbf{q}$ at every node converges to the same value. Note from (8) that the optimization problem (11) can be rewritten as a quadratic optimization problem, which can be solved using standard quadratic programming solvers.

In the following section, we investigate the assumptions under which the proposed distributed EM algorithm converges.

IV. CONVERGENCE ANALYSIS

We require the following technical assumptions to show that the proposed distributed EM algorithm converges. These assumptions are similar to those in [21], [22], which however requires that (7) belongs to the exponential family. The main difference with [21], [22] is the following:

we show that despite optimizing the single-parameter log-likelihood functions (5)-(6) separately, the overall solution of the different sensors converge to the same solution.

Assumption 1 *There are convex open subsets $\mathcal{S}$ and $\mathcal{T}$ such that:*

(a) for any $s_i \in \mathcal{S}$, and $\lambda \in [0,1]$, $(1 - \lambda)s_i + \lambda \bar{s}_i(\mathbf{x})) \in \mathcal{S}$; for any $t_i \in \mathcal{T}$, and $\lambda \in [0,1]$, $(1 - \lambda)t_i + \lambda \bar{t}_i(\mathbf{x})) \in \mathcal{T}$.

(b) for any $s_i \in \mathcal{S}$, the function $\mathbf{q} \mapsto s_i^T \phi_1(\mathbf{q})$ has a unique global maximum denoted by $\bar{\mathbf{q}}(s_i)$; for any $t_i \in \mathcal{T}$, the function $\theta_1 \mapsto t_i^T \phi_2(\theta_1)$ has a unique global maximum denoted by $\bar{\theta}_1(t_i)$; for any $s_i \in \mathcal{S}$, any $t_i \in \mathcal{T}$, the function $\theta_i \mapsto \bar{\psi}_i(\theta_i, \bar{\mathbf{q}}(s_i), \bar{\theta}_1(t_i); \mathbf{x}^{n-1})$ has a unique global maximum.

Note that Assumption 1(b) may not hold when $\bar{\mathbf{q}}(s)$ or $\bar{\theta}_1(t)$ hit the boundaries of its domain. In addition, Assumption 1(a) is hard to verify in practice. Therefore, it is of common practice to confine $\tilde{s}_i$ and $\tilde{t}_i$ in the updating step (9) to the given convex sets $\mathcal{S}$ and $\mathcal{T}$ by projection. The projection procedure does not affect the convergence analysis.

Assumption 2 *The step sizes λ_n are chosen so that $\sum_{n=1}^{\infty} \lambda_n = \infty$ and $\sum_{n=1}^{\infty} \lambda_n^2 < \infty$.*

Assumption 3 *The weighting matrix has the following properties.*

(a) For any n, $W_n \triangleq [w_n(i,j)]_{i,j=2...N}$ is a matrix-valued random variable with non negative elements.

(b) For any n, W_n is row stochastic : $W_n \mathbf{1} = \mathbf{1}$.

(c) W_n is column stochastic in expectation: $\mathbb{E}(W_n)^T \mathbf{1} = \mathbf{1}$.

(d) $\{W_n\}_{n \geq 1}$ is an independent identically distributed sequence.

(e) The spectral norm ρ of matrix $\mathbb{E}(W_n^T(I_N - \mathbf{1}\mathbf{1}^T/N)W_n)$ satisfies $\rho < 1$

Finally, let us define $K(\mathbf{x})$ as

$$K(\mathbf{x}) \triangleq \log \int p\left(\{\tilde{d}_{i1}, \tilde{\theta}_i, \gamma_i\}_{i=2}^N, \tilde{\theta}_1 \,\middle|\, \mathbf{x}\right) \mathrm{d}\gamma_2 \ldots, \gamma_N \tag{14}$$

We let $\mathcal{E} = \{\mathbf{x} : \nabla_{\mathbf{x}} K(\mathbf{x}) = 0\}$. The following result shows that the sequence $\mathbf{x}_i^n$ in our distributed EM algorithm converges to the same local maximizer for all sensors.

Theorem 1 *Under Assumptions 1, 2 and 3, we have $\lim_{n \to \infty} \max_{i,j=2...N} \|\mathbf{x}_i^n - \mathbf{x}_j^n\| = 0$ with probability 1 and $\lim_{n \to \infty} d(\mathbf{x}_i^n, \mathcal{E}) = 0$ with probability 1 for $i = 2, \ldots, N$.*

We provide an outline for the proof of Theorem 1 below, largely based on the proof of Theorem 1 in [29]. The full proof is provided in Appendix B.

(i) We start by showing that the nodes asymptotically reach a consensus on their estimate, i.e., $\lim_{n\to\infty} \max_{i,j=2\ldots N} \left\| \mathbf{x}_i^n - \mathbf{x}_j^n \right\| = 0$ with probability 1. Therefore, the convergence analysis of the vectors $\mathbf{s}_n = \text{Vec}(\{s_i^n\}_{i=2}^N)$ and $\mathbf{t}_n = \text{Vec}(\{t_i^n\}_{i=2}^N)$ reduces to analyzing the average estimates $\langle \mathbf{s}_n \rangle$ and $\langle \mathbf{t}_n \rangle$ (see Lemma 1 in [29]).

(ii) We show that $\langle \mathbf{s}_n \rangle$ and $\langle \mathbf{t}_n \rangle$ follow the following time-dynamical system:

$$\langle \mathbf{s}_n \rangle = \langle \mathbf{s}_{n-1} \rangle + \lambda_n h_1(\langle \mathbf{s}_{n-1} \rangle, \langle \mathbf{t}_{n-1} \rangle) + \lambda_n \xi_1^n + \lambda_n r_1^n$$

$$\langle \mathbf{t}_n \rangle = \langle \mathbf{t}_{n-1} \rangle + \lambda_n h_2(\langle \mathbf{s}_{n-1} \rangle, \langle \mathbf{t}_{n-1} \rangle) + \lambda_n \xi_2^n + \lambda_n r_2^n$$

where $h_1(\cdot, \cdot)$ and $h_2(\cdot, \cdot)$ are two functions defined in (17), while ξ_l^n and r_l^n for $l = 1, 2$ are error terms given by (19). These equations can be viewed as noisy approximations of the following Ordinary Differential Equation (ODE):

$$\dot{s} = h_1(s, t)$$

$$\dot{t} = h_2(s, t)$$

We show that the roots of h_1 and h_2 correspond to a stationary point of $\mathbf{x} \mapsto K(\mathbf{x})$.

(iii) We then show that the sequence of $\mathbf{x}_i^n$ converges to the same local maximizers for all nodes.

(iv) Finally, we show that the terms $\lambda_n \xi_1^n$, $\lambda_n \xi_2^n$, $\lambda_n r_1^n$ and $\lambda_n r_2^n$ asymptotically tend to 0 with probability 1.

By combining these results, we show that our distributed EM algorithm converges to the same local maximizer for all nodes.

V. SIMULATION RESULTS

In this section, we present simulation results to verify the performance of our proposed distributed EM algorithm. In our simulations, we use the pairwise gossip scheme [30] in the Gossip Step of the distributed EM algorithm. Specifically, at each iteration, two neighboring nodes i and j are randomly chosen to compute the weighted averages $s_i^n = s_j^n = 0.5\tilde{s}_i^n + 0.5\tilde{s}_j^n$ and $t_i^n = t_j^n = 0.5\tilde{t}_i^n + 0.5\tilde{t}_j^n$. For other nodes $k \notin \{i, j\}$, $s_k^n = \tilde{s}_k^n$ and $t_k^n = \tilde{t}_k^n$.

We compare the performances of the proposed distributed algorithm with the centralized algorithm, as well as with the algorithm proposed in [14]. The algorithm in [14] is adapted to

use TDOA measurements rather than TOA measurements (and does not make use of the AOA information). In practice, [14] estimates the noise probability density function (which can be non-central or multi-modal) of the different measurements along with the target location. As the TDOA measurement noise is allowed to be non-central, the algorithm in [14] allows us to account for the bias in the NLOS measurements. The method of [14] requires the use of several independent measurements, which we set to 10 to match our later experimental results.
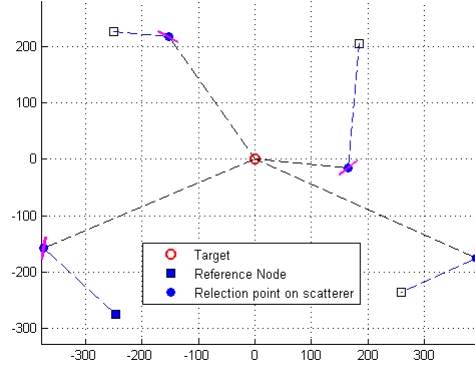

Fig. 4. Configuration of sensors and the target. The dotted lines denote the signal paths between the target and sensors.
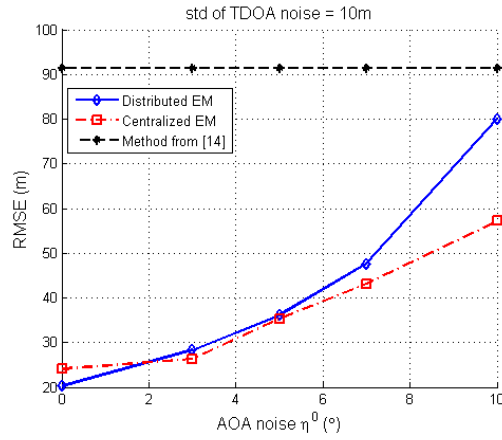

Fig. 5. RMSE of the estimated target position versus angle noise η^0, with $\sigma_i = 10$m, $i = 1, \ldots, N$.

The simulated scenario is shown in Fig. 4. The square markers represent the sensors. Taking the support set of γ_i in our algorithm to be $[\gamma_i^0 - 10°, \gamma_i^0 + 10°]$, where γ_i^0 is the true scatterer orientation, the angle noise η_i uniformly distributed in $[-\eta^0, \eta^0]$, and the TDOA measurement noise to be zero-mean Gaussian, the root mean square error (RMSE) of the estimated target
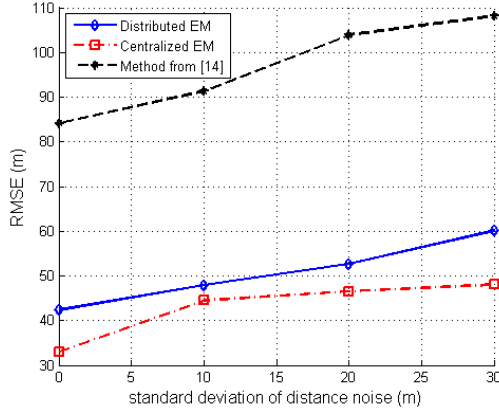
Fig. 6. RMSE of the estimated target position versus standard deviation of distance noise σ_i, with $\eta^0 = 7°$.

position is shown in Fig. 5 and Fig. 6. Comparing the performances of our distributed EM algorithm and the method from [14], it is observed that the localization accuracy is greatly improved by using the additional AOA information. It is also seen that our proposed algorithm has similar performance as that of the centralized EM method, except when the measurement noises become large. One reason that the algorithm of [14] performs so poorly is because [14] assumes that the TDOA noise of *all* measurements are i.i.d. realizations from an identical noise pdf (which can be non-zero-mean to account for NLOS). In a NLOS situation, each TDOA measurement will have a distinct non-zero mean compared to the LOS case, which will be different for each pair of nodes, rendering the i.i.d. assumption invalid and deteriorating the performances of the method in [14].

VI. EXPERIMENTAL RESULTS

In this section, we evaluate the performance of the distributed EM algorithm in an experimental setting. We start by describing the measurement setup, and then analyze the localization performance. Note that the TDOA and AOA measurements are separate experiments, performed with the nodes placed in identical locations. The TDOA and AOA at each node are extracted from the measurements for each transmitter location, and fused off-line to evaluate the performance of the distributed EM algorithm.

A. Measurement setup

We consider a network of 1 transmitting target and 4 sensor nodes, located on different floors of a building facing another building about 40 m away. The transmitter and one of the sensors (S_1) are placed on a corridor on the same floor with a clear LOS. Another sensor (S_3) is placed on the same floor as the transmitter, but behind a corner in a NLOS situation. The signal path from the transmitter to S_3 is expected to be a diffracted path around the corner. Although this signal path does not have a single reflection from a scatterer, as assumed in our system model, the diffracted path can nevertheless be modeled as a reflected path off a virtual scatterer near the corner. Two of the sensors, S_2 and S_4, are placed on a different floor so that the signal path from the target to each of these nodes consist of a NLOS path bounced off the opposite building (see Figure 7). The transmitter was moved along 13 different measurement locations along a line going from S_1 towards S_3. The transmitter is moved to 13 different measurement locations

Fig. 7. Picture of the measurement site. The two NLOS nodes are placed on a different floor than the transmitter and the LOS node. The node S_3 is around a corner of the corridor in which the transmitter is placed.

along a line, as shown in Figure 7. The distance between node S_1 and and the corridor leading
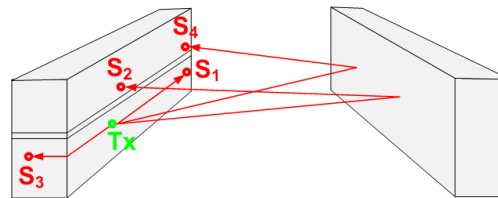

Fig. 8. Expected signal paths between the transmitter and the different receiver nodes.

to S_3 is 100 m, and the distance between nodes S_2 and S_4 is 50 m. The longest path between any transmitter location and any receiver is 106 m. The largest measured TDOA is 160 m. The building opposite the measurement building is approximately 40 m away.

AOA measurement: A 4-channel Pentek 4995A A/D converter is used as a 4-element MIMO receiver. The A/D converter is able to sample signals up to 200 MHz, and is used as a sub-sampled receiver by connecting the antennas straight to the A/D converter [31]. The source signal is generated with a signal generator sending a pilot tone at 795 MHz. The four antennas of the receiver form a linear array with a distance of 15 cm between antennas. We use the well-known Multiple Signal Classification (MUSIC) algorithm to recover the AOA of the signal paths [32]. For a 4-element array, the MUSIC algorithm is able to recover up to three signal paths, even though in our experiment, there is only be one dominant path from the target to each sensor node. The receiver has been carefully calibrated, and measurements in an anechoic chamber show that our setup has an zero-mean AOA error with a standard deviation of $3°$. Our AOA measurements confirm that for nodes S_2 and S_4, the dominant path from the transmitter to the NLOS nodes occurs through a reflection on the building opposite the receiver nodes. For node S_3, the measurement confirm that the dominant path comes through diffraction around the corner of the building.

TDOA measurement: We use a USRP software-defined radio platform to measure the TDOA between different nodes. The USRPs are equipped with WBX daughterboards and a GPSDO module, which synchronizes the internal clock and local oscillator of the different nodes to the GPS UTC time [33]. However, even with GPS synchronization, the time offset between the different nodes can still be as large as 100 ns, causing TDOA errors up to 60 m. To improve on this, we use a simple relaying architecture described in Appendix C. We characterize our TDOA measurement setup by measuring the TDOA between different nodes in an ideal environment (with cables, no multipath and high SNR) and find that the TDOA measurement error is as small as 3 m. In outdoor line-of-sight environments, the TDOA error of our setup has a mean of 1 m and a standard deviation of 4 m. For each transmitter location, 10 TDOA measurements are taken. Similarly as for the AOA measurement, the measured values for our TDOA indicate that for the NLOS nodes the dominant path occurs through a reflection on the building opposite the receiver nodes or through diffraction around the corner of the building. All the parameters of our setup are given in Appendix C. We stress that our TDOA measurement setup *does not* aim at reproducing the distributed EM algorithm, but is used to measure the TDOA between different pair of nodes so that the distributed EM algorithm can be evaluated over real measurements offline.

B. Localization results

For each of the 13 target locations, we make ten TDOA measurements and one AOA measurement. We use the distributed EM algorithm to determine the location of the target for each of these 13×10 measurements. We also compute the location estimate with the centralized EM algorithm to serve as a benchmark. The distributed and centralized algorithms require initial estimates for the transmitter location. The initial guess can be set randomly, and is set to $(0, 0)$ (in the frame of reference of Figure 9) for all our measurements. The termination conditions for the centralized EM algorithm is the following: once the difference in the transmitter's location estimate between two successive iterations reaches below a certain threshold, the algorithm is supposed to have converged. The distributed EM algorithm is supposed to have converged once the difference between the transmitter's location estimate at the different senors reaches below a certain threshold. In both cases, the threshold is set to 1 m. Figure 9 shows an example of the algorithm results for one particular transmitter location. In this case, the scatterer angle support set was chosen to be $[\gamma_i^0 - 10°, \gamma_i^0 + 10°]$, where γ_i^0 is the true scatterer orientation. Even though the algorithm does not know the building location, it is able to obtain a fair estimate of the scatterer locations, and to estimate the target location. It can be observed how the LOS node
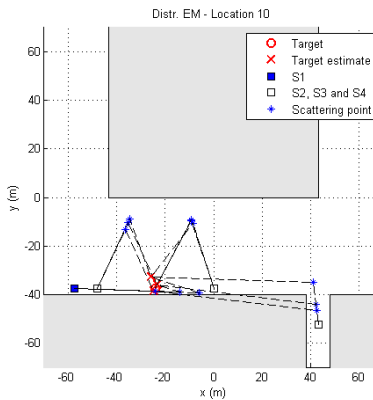

Fig. 9. Localization result when using the distributed EM algorithm. The scatterer angle support set was chosen to be $[\gamma_i^0 - 10°, \gamma_i^0 + 10°]$.

S_1 is treated exactly as a NLOS node. In that case, the algorithm chooses a scatterer whose orientation is parallel to the line between transmitter and LOS node.

Assuming knowledge of the scatterer orientation angle may be an unrealistic assumption in many scenarios. Figure 10 shows an example of the algorithm output when the scatterer angle

support set was chosen to be $[0°, 90°, 135°, 180°, 270°]$. In this scenario, the possible scatterer orientation angles are limited to a finite set, which is a fairly realistic assumption in environments with symmetric geometries (e.g. cities with regular city blocks). It can be seen that this scenario the distributed EM algorithm is able to successfully locate the RF target.
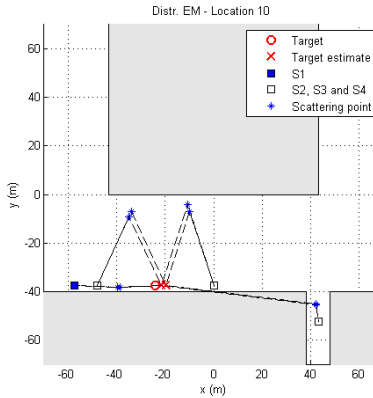

Fig. 10. Localization result when using the distributed EM algorithm. The scatterer angle support set was chosen to be $[0°, 90°, 135°, 180°, 270°]$.

Figure 11 shows the localization error over all measurements, both for the centralized and distributed EM (the results for the two types of scatterer angle support sets are shown). Note that for the distributed EM, the algorithm could converge in 82% of the measurements, while for the centralized EM, the algorithm could always converge. When the distributed EM algorithm converges, it typically does so in less than 20 iterations (meaning there are at most 20 message exchanges between the different nodes). The cases where the distributed EM could not converge correspond to cases where the TDOA and/or AOA measurements are very bad, and the estimates of the different nodes diverge too strongly for the algorithm to converge to a unique solution. In the centralized case, these measurements just result in poor localization accuracy. In Figure 11, the measurements with large errors in the centralized EM algorithm correspond to the measurements for which our distributed EM algorithm could not find a solution, which explains why the distributed EM slightly outperforms the centralized EM. For all measurements, the localization error is below 15 m. We also evaluated the performances of the method proposed in [14] for comparison. Similarly to the simulated case, it can be observed that the error of [14] is much larger than the one in our proposed method. This is due to the fact that [14] assumes that the NLOS aspect of the TDOA measurements can be treated as a non-zero-mean noise, but

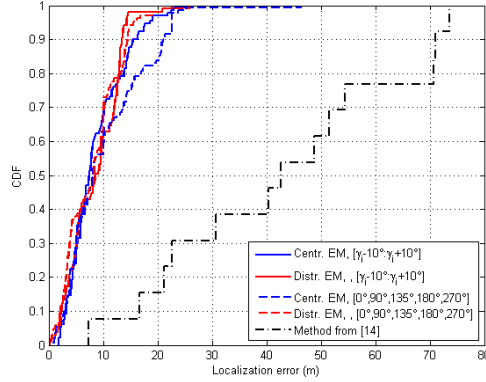[14] requires that all the TDOA measurements have the same noise pdf, which is not the case in practice.

Fig. 11. Cumulative distribution function of the localization error, both for the centralized and distributed EM algorithm for two types of scatterer angle support set.

VII. CONCLUSION

In this work, we propose a distributed EM algorithm for target localization in NLOS environments. We provide sufficient conditions for the proposed algorithm to converge, and prove its convergence. Simulation results show that additional AOA information which is utilized in the proposed EM algorithm significantly improves localization accuracy. When applying the distributed EM algorithm to experimental measurements, it is observed that the algorithm is able to localize a target with an accuracy below 15 m, and has errors similar to a centralized EM approach, verifying that our algorithm works when applied to realistic environments.

APPENDIX A
SCATTERING ANGLES OF A SINGLE-BOUNCE REFLECTION

In this section, we show that $\phi_i = 2\gamma_i - \theta_i$, where θ_i is the AOA at sensor i, γ_i is the orientation of the reflector of sensor i, and ϕ_i is the angle of the vector with direction opposite of the AOD. This can be deduced from Snell's law of reflection, which states that the angle of incidence is equal to the angle of reflection. Consider Figure 12, where the green line is perpendicular to the scatterer. The angle of incidence can be expressed as

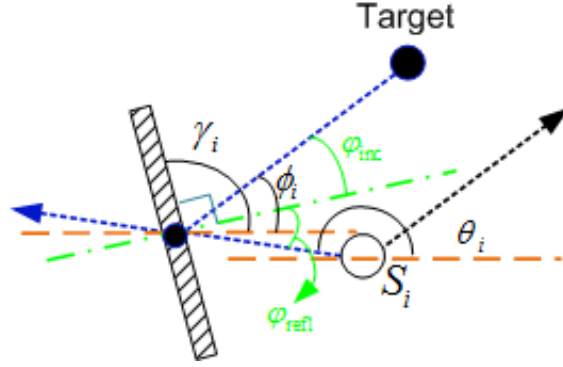$$\varphi_{\text{inc}} = \phi_i - (\gamma_i - \pi/2)$$

Fig. 12. Detailed view of the reflection from target to sensor.

The angle of reflection can be expressed as

$$\varphi_{\text{refl}} = (\pi - \theta_i) + (\gamma_i - \pi/2)$$

Since Snell's law of reflection states that $\varphi_{\text{inc}} = \varphi_{\text{refl}}$, we obtain that $\phi_i = 2\gamma_i - \theta_i$.

APPENDIX B

PROOF OF THEOREM 1

In this section we provide a proof for Theorem 1, based on the outline detailed in Section IV. In the sequel, we will use following notations. We let $\mathbf{s}_n = \text{Vec}(\{s_i^n\}_{i=2}^N)$, $\mathbf{t}_n = \text{Vec}(\{t_i^n\}_{i=2}^N)$, $\mathbf{A}_n = \text{Vec}(\{\bar{s}_i(\mathbf{x}_i^{n-1}) - s_i^{n-1}\}_{i=2}^N)$ and $\mathbf{B}_n = \text{Vec}(\{\bar{t}_i(\mathbf{x}_i^{n-1}) - t_i^{n-1}\}_{i=2}^N)$. Then the local step (9) and gossip step (10) can be combined as

$$\mathbf{s}_n = (W_n \otimes I_{d_s})[\mathbf{s}_{n-1} + \lambda_n \mathbf{A}_n] \tag{15a}$$

$$\mathbf{t}_n = (W_n \otimes I_{d_t})[\mathbf{t}_{n-1} + \lambda_n \mathbf{B}_n] \tag{15b}$$

The following lemma follows directly from Lemma 1 of [29]. It shows that nodes asymptotically reach a consensus on their estimate. Therefore, the convergence analysis of the vector $\mathbf{s}_n$ and $\mathbf{t}_n$ reduce to an analysis of the average estimates $\langle \mathbf{s}_n \rangle$ and $\langle \mathbf{t}_n \rangle$.

Lemma 1 *Under Assumptions 1, 2 and 3, we have $\max_{i,j=2...N} \left\| s_i^n - s_j^n \right\|$ and $\max_{i,j=2...N} \left\| t_i^n - t_j^n \right\|$ converging to zero a.s. as n tends to infinity.*

A. Discrete-time dynamical system of $\langle \mathbf{s}_n \rangle$ and $\langle \mathbf{t}_n \rangle$

We now proceed to the analysis of the average estimates $\langle \mathbf{s}_n \rangle$ and $\langle \mathbf{t}_n \rangle$. The terms $\langle \mathbf{s}_n \rangle$ and $\langle \mathbf{t}_n \rangle$ follow the below discrete time dynamical system:

$$\langle \mathbf{s}_n \rangle = \langle \mathbf{s}_{n-1} \rangle + \lambda_n h_1(\langle \mathbf{s}_{n-1} \rangle, \langle \mathbf{t}_{n-1} \rangle) + \lambda_n \xi_1^n + \lambda_n r_1^n \tag{16a}$$

$$\langle \mathbf{t}_n \rangle = \langle \mathbf{t}_{n-1} \rangle + \lambda_n h_2(\langle \mathbf{s}_{n-1} \rangle, \langle \mathbf{t}_{n-1} \rangle) + \lambda_n \xi_2^n + \lambda_n r_2^n \tag{16b}$$

with

$$h_1(s,t) \triangleq \bar{s}(\bar{\mathbf{q}}(s), \bar{\theta}_1(t)) - s \tag{17a}$$

$$h_2(s,t) \triangleq \bar{t}(\bar{\mathbf{q}}(s), \bar{\theta}_1(t)) - t \tag{17b}$$

$$\bar{s}(\bar{\mathbf{q}}(s), \bar{\theta}_1(t)) \triangleq \frac{1}{N-1} \sum_{i=2}^{N} \bar{s}_i(\bar{\mathbf{q}}(s), \bar{\theta}_1(t)) \tag{18a}$$

$$\bar{t}(\bar{\mathbf{q}}(s), \bar{\theta}_1(t)) \triangleq \frac{1}{N-1} \sum_{i=2}^{N} \bar{t}_i(\bar{\mathbf{q}}(s), \bar{\theta}_1(t)) \tag{18b}$$

$$\xi_1^n = \frac{1}{(N-1)\lambda_n} [(\mathbf{1}^T W_n - \mathbf{1}^T) \otimes I_{d_s}][\mathbf{s}_{n-1} + \lambda_n \mathbf{A}_n] \tag{19a}$$

$$r_1^n = \frac{1}{N-1} \sum_{i=2}^{N} (\bar{s}_i(\bar{\mathbf{q}}(s_i^n), \bar{\theta}_1(t_i^n)) - s_i^n) - h_1(\langle \mathbf{s}_{n-1} \rangle, \langle \mathbf{t}_{n-1} \rangle) \tag{19b}$$

$$\xi_2^n = \frac{1}{(N-1)\lambda_n} [(\mathbf{1}^T W_n - \mathbf{1}^T) \otimes I_{d_t}][\mathbf{t}_{n-1} + \lambda_n \mathbf{B}_n] \tag{19c}$$

$$r_2^n = \frac{1}{N-1} \sum_{i=1}^{N} (\bar{t}_i(\bar{\mathbf{q}}(s_i^n), \bar{\theta}_1(t_i^n)) - t_i^n) - h_2(\langle \mathbf{s}_{n-1} \rangle, \langle \mathbf{t}_{n-1} \rangle) \tag{19d}$$

The discrete time dynamical system above can be viewed as a noisy approximation of the following ordinary differential equation (ODE),

$$\dot{s} = h_1(s,t) \tag{20a}$$

$$\dot{t} = h_2(s,t) \tag{20b}$$

where $\dot{s}$ and $\dot{t}$ respectively denote the derivative of s and t with respect to time. The following proposition shows that

$$w(s,t) \triangleq -K(\bar{\mathbf{q}}(s), \bar{\theta}_1(t))$$

is a Lyapunov function of the ODE (20). In other works, Proposition 1 shows that the roots of h_1 and h_2 correspond to a stationary point of $\mathbf{x} \mapsto K(\mathbf{x})$, i.e., $\nabla_{\mathbf{x}} K(\mathbf{x})|_{\mathbf{x}=\mathbf{x}^*} = 0$;

Proposition 1 *Under Assumptions 1 and 2, if (s^*, t^*) is such that $h_1(s^*, t^*) = 0$ and $h_2(s^*, t^*) = 0$, then $\mathbf{x}^* = [\bar{\mathbf{q}}(s^*); \bar{\theta}_1(t^*)]$ is a stationary point of $\mathbf{x} \mapsto K(\mathbf{x})$, i.e., $\nabla_{\mathbf{x}} K(\mathbf{x})|_{\mathbf{x}=\mathbf{x}^*} = 0$. Conversely, for any $\mathbf{x}^* = [\mathbf{q}^*; \theta_1^*]$, such that $\nabla_{\mathbf{x}} K(\mathbf{x})|_{\mathbf{x}=\mathbf{x}^*} = 0$, we have $s^* = \bar{s}(\mathbf{x}^*)$, $t^* = \bar{t}(\mathbf{x}^*)$ satisfy $h_1(s^*, t^*) = 0$ and $h_2(s^*, t^*) = 0$.*

Proof: To simplify notations, let $\mathbf{x}^* = [\mathbf{q}^*; \theta_1^*]$ with $\mathbf{q}^* = \bar{\mathbf{q}}(s^*)$ and $\theta_1^* = \bar{\theta}_1(t^*)$. Since the function $\mathbf{q} \mapsto \phi_1^T(\mathbf{q})s$ has a unique global maximum at $\bar{\mathbf{q}}(s)$ and $\theta_1 \mapsto \phi_2^T(\theta_1)t$ has a unique global maximum at $\bar{\theta}_1(t)$ (cf. Assumption 1(c)), we obtain

$$\nabla_{\mathbf{q}} \phi_1^T(\mathbf{q}^*)s^* = 0, \quad \nabla_{\theta_1} \phi_2^T(\theta_1^*)t^* = 0. \tag{21}$$

From Fisher's identity [19], we have

$$\nabla_{\mathbf{x}} K(\mathbf{x}) = \int \left\{ \nabla_{\mathbf{x}} \log p\left(\{\tilde{d}_{i1}, \theta_i, \gamma_i\}_{i=2}^N, \tilde{\theta}_i \,\middle|\, \mathbf{x} \right) \right\} \mathrm{d}\gamma_2 \dots, \gamma_N \mathrm{d}\theta_2 \dots, \theta_N$$

$$= (N-1) \begin{bmatrix} \nabla_{\mathbf{q}} \phi_1^T(\mathbf{q})\bar{s}(\mathbf{x}) \\ \nabla_{\theta_1} \phi_2^T(\theta_1)\bar{t}(\mathbf{x}) \end{bmatrix} \tag{22}$$

where the $N-1$ factor arises because $\bar{s}$ and $\bar{t}$ defined in (18) are normalized by $N-1$. Without loss of generality, we will omit the factor $N-1$ for conciseness.

Since $h_1(s^*, t^*) = 0$ and $h_2(s^*, t^*) = 0$, i.e., $s^* = \bar{s}(\mathbf{x}^*)$, $t^* = \bar{t}(\mathbf{x}^*)$, (21) and (22) imply that

$$\nabla_{\mathbf{x}} K(\mathbf{x})|_{\mathbf{x}=\mathbf{x}^*} = \begin{bmatrix} \nabla_{\mathbf{q}} \phi_1^T(\mathbf{q}^*)s^* \\ \nabla_{\theta_1} \phi_2^T(\theta_1^*)t^* \end{bmatrix} = 0$$

and the forward part is proved.

Conversely, let $\mathbf{x}^* = [\mathbf{q}^*; \theta_1^*]$, $s^* = \bar{s}(\mathbf{x}^*)$ and $t^* = \bar{t}(\mathbf{x}^*)$. Assuming $\nabla_{\mathbf{x}} K(\mathbf{x})|_{\mathbf{x}=\mathbf{x}^*} = 0$, then by (22) we have

$$\nabla_{\mathbf{q}} \phi_1^T(\mathbf{q}^*)s^* = 0, \quad \nabla_{\theta_1} \phi_2^T(\theta_1^*)t^* = 0$$

Under Assumption 1(b), the function $\mathbf{q} \mapsto \phi_1^T(\mathbf{q})s^*$ and $\theta_1 \mapsto \phi_2^T(\theta_1)t^*$ has a unique global maximum at $\bar{\mathbf{q}}(s^*)$ and $\bar{\theta}_1(t^*)$, respectively. Hence, $\mathbf{q}^* = \bar{\mathbf{q}}(s^*)$ and $\theta_1^* = \bar{\theta}_1(t^*)$ and the converse part is proved. The proof of the Proposition 1 is now complete. ∎

B. Identical local maximizer for all nodes

Let us define $h(s,t) = [h_1(s,t)^T, h_2(s,t)^T]^T$ and $\nabla_{s,t} w(s,t) = [\nabla_s^T w(s,t), \nabla_t^T w(s,t)]^T$.

Proposition 2 *Suppose that Assumptions 1 and 2 hold, and $w(s,t)$ is continuously differentiable on $\mathcal{S} \times \mathcal{T}$. Then, $\langle \nabla_{s,t} w(s,t), h(s,t) \rangle \leq 0$ and $\langle \nabla_{s,t} w(s,t), h(s,t) \rangle = 0$ if and only if $h(s,t) = 0$.*

Proof: The inner product between $\nabla_{s,t} w(s,t)$ and $h(s,t)$ can be written as

$$\langle \nabla_{s,t} w(s,t), h(s,t) \rangle = h_1^T(s,t) \nabla_s w(s,t) + h_2^T(s,t) \nabla_t w(s,t) \tag{23}$$

Let $\bar{\mathbf{x}}(s,t) = [\bar{\mathbf{q}}^T(s), \bar{\theta}_1(t)]^T$. Using (22) and the chain rule of differentiation,

$$\nabla_s w(s,t) = -\nabla_s \bar{\mathbf{x}}^T(s,t) \nabla_{\mathbf{x}} K(\mathbf{x})|_{\mathbf{x} = \bar{\mathbf{x}}(s,t)}$$

$$= -\nabla_s \bar{\mathbf{x}}^T(s,t) \begin{bmatrix} \nabla_{\mathbf{q}} \phi_1^T \{\bar{\mathbf{q}}(s)\} \bar{s}(\bar{\mathbf{x}}(s,t)) \\ \nabla_{\theta_1} \phi_2^T \{\bar{\theta}_1(t)\} \bar{t}(\bar{\mathbf{x}}(s,t)) \end{bmatrix} \tag{24}$$

Let $l_1(s; \mathbf{q}) = \phi_1^T(\mathbf{q})s$ and $l_2(t; \theta_1) = \phi_2^T(\theta_1)t$. Note that since $\bar{\mathbf{q}}(s)$ and $\bar{\theta}_1(t)$ are the maximum of $\mathbf{q} \mapsto l_1(s; \mathbf{q})$ and $\theta_1 \mapsto l_2(t; \theta_1)$, respectively, we have

$$\nabla_{\mathbf{q}} \phi_1^T \{\bar{\mathbf{q}}(s)\} s = 0, \tag{25a}$$

$$\nabla_{\theta_1} \phi_2^T \{\bar{\theta}_1(t)\} t = 0. \tag{25b}$$

Using definition of $h_1(s,t)$ and $h_2(s,t)$ given in (17) and substituting into (24), we obtain

$$\nabla_s w(s,t) = -\left[\nabla_s \bar{\mathbf{q}}^T(s) \nabla_{\mathbf{q}} \phi_1^T \{\bar{\mathbf{q}}(s)\} h_1(s,t) + \nabla_s \bar{\theta}_1^T(t) \nabla_{\theta_1} \phi_2^T \{\bar{\theta}_1(t)\} h_2(s,t)\right] \tag{26}$$

Differentiating the function $s \mapsto \Phi_1\{s, \bar{\mathbf{q}}(s)\}$ where $\Phi_1(s, \mathbf{q}) \triangleq \nabla_{\mathbf{q}} l_1(s; \mathbf{q})$, we have

$$\nabla_s \Phi_1^T \{s, \bar{\mathbf{q}}(s)\} = \nabla_s \Phi_1^T(s, \mathbf{q})_{\mathbf{q} = \bar{\mathbf{q}}(s)} + \nabla_s \bar{\mathbf{q}}^T(s) \nabla_{\mathbf{q}} \Phi_1^T(s, \mathbf{q})_{\mathbf{q} = \bar{\mathbf{q}}(s)}.$$

Since $\nabla_s \Phi_1^T(s, \mathbf{q}) = \nabla_s (\nabla_{\mathbf{q}} l_1(s; \mathbf{q}))^T = (\nabla_{\mathbf{q}} \phi_1^T(\mathbf{q}))^T$ and $\nabla_{\mathbf{q}} \Phi_1^T(s, \mathbf{q}) = \nabla_{\mathbf{q}}^2 l_1(s; \mathbf{q})$, the above equation can be rewritten as

$$\nabla_s (\nabla_{\mathbf{q}} l_1(s; \mathbf{q})|_{\mathbf{q} = \bar{\mathbf{q}}(s)})^T = (\nabla_{\mathbf{q}} \phi_1^T \{\bar{\mathbf{q}}(s)\})^T + \nabla_s \bar{\mathbf{q}}^T(s) \nabla_{\mathbf{q}}^2 l_1(s; \mathbf{q})|_{\mathbf{q} = \bar{\mathbf{q}}(s)}.$$

Because $\nabla_{\mathbf{q}} l_1(s; \mathbf{q})|_{\mathbf{q} = \bar{\mathbf{q}}(s)} = 0$, we get

$$\nabla_{\mathbf{q}} \phi_1^T \{\bar{\mathbf{q}}(s)\} = -\nabla_{\mathbf{q}}^2 l_1(s; \mathbf{q})|_{\mathbf{q} = \bar{\mathbf{q}}(s)} (\nabla_s \bar{\mathbf{q}}^T(s))^T.$$

Following similar arguments as above, we have

$$\nabla_{\theta_1} \phi_2^T \{\bar{\theta}_1(t)\} = -\nabla_{\theta_1}^2 l_2(t; \theta_1)|_{\theta_1 = \bar{\theta}_1(t)} (\nabla_t \bar{\theta}_1^T(t))^T.$$

Plugging the above two equations into (26) and noting that $\nabla_s \bar{\theta}_1(t) = \nabla_s t^T \nabla_t \bar{\theta}_1(t)$, we have

$$h_1^T(s,t)\nabla_s w(s,t) = h_1^T(s,t)(\nabla_{\mathbf{q}}\phi_1^T\{\bar{\mathbf{q}}(s)\})^T\{\nabla_{\mathbf{q}}^2 l_1(s;\mathbf{q})|_{\mathbf{q}=\bar{\mathbf{q}}(s)}\}^{-1}\nabla_{\mathbf{q}}\phi_1^T\{\bar{\mathbf{q}}(s)\}h_1(s,t)$$
$$+ h_1^T(s,t)\nabla_s t^T(\nabla_{\theta_1}\phi_2^T\{\bar{\theta}_1(t)\})^T\{\nabla_{\theta_1}^2 l_2(t;\theta_1)|_{\theta_1=\bar{\theta}_1(t)}\}^{-1}\nabla_{\theta_1}\phi_2^T\{\bar{\theta}_1(t)\}h_2(s,t)$$

Using similar arguments as above, we can also show that

$$h_2^T(s,t)\nabla_t w(s,t) = h_2^T(s,t)\nabla_t s^T(\nabla_{\mathbf{q}}\phi_1^T\{\bar{\mathbf{q}}(s)\})^T\{\nabla_{\mathbf{q}}^2 l_1(s;\mathbf{q})|_{\mathbf{q}=\bar{\mathbf{q}}(s)}\}^{-1}\nabla_{\mathbf{q}}\phi_1^T\{\bar{\mathbf{q}}(s)\}h_1(s,t)$$
$$+ h_2^T(s,t)(\nabla_{\theta_1}\phi_2^T\{\bar{\theta}_1(t)\})^T\{\nabla_{\theta_1}^2 l_2(t;\theta_1)|_{\theta_1=\bar{\theta}_1(t)}\}^{-1}\nabla_{\theta_1}\phi_2^T\{\bar{\theta}_1(t)\}h_2(s,t)$$

Using the ODE given in (20), we have $h_1^T(s,t)\nabla_s t^T = \dot{s}^T\nabla_s t^T = 2\dot{t} = 2h_2^T(s,t)$ and similarly, $h_2^T(s,t)\nabla_t s^T = 2h_1^T(s,t)$.

Therefore, $\langle \nabla_{s,t} w(s,t), h(s,t)\rangle$ can be expressed as

$$\langle \nabla_{s,t} w(s,t), h(s,t)\rangle$$
$$= 3h_1^T(s,t)(\nabla_{\mathbf{q}}\phi_1^T\{\bar{\mathbf{q}}(s)\})^T\{\nabla_{\mathbf{q}}^2 l_1(s;\mathbf{q})|_{\mathbf{q}=\bar{\mathbf{q}}(s)}\}^{-1}\nabla_{\mathbf{q}}\phi_1^T\{\bar{\mathbf{q}}(s)\}h_1(s,t)$$
$$+ 3h_2^T(s,t)(\nabla_{\theta_1}\phi_2^T\{\bar{\theta}_1(t)\})^T\{\nabla_{\theta_1}^2 l_2(t;\theta_1)|_{\theta_1=\bar{\theta}_1(t)}\}^{-1}\nabla_{\theta_1}\phi_2^T\{\bar{\theta}_1(t)\}h_2(s,t) \qquad (27)$$

where Assumption 1(b) implies that the matrices $\nabla_{\mathbf{q}}^2 l_1(s;\mathbf{q})|_{\mathbf{q}=\bar{\mathbf{q}}(s)}$ and $\nabla_{\theta_1}^2 l_2(t;\theta_1)|_{\theta_1=\bar{\theta}_1(t)}$ are negative definite. Therefore, $\langle \nabla_{s,t} w(s,t), h(s,t)\rangle \leq 0$ with equality if and only if $\nabla_{\mathbf{q}}\phi_1^T\{\bar{\mathbf{q}}(s)\}h_1(s,t) = 0$ and $\nabla_{\theta_1}\phi_2^T\{\bar{\theta}_1(t)\}h_2(s,t) = 0$. Assuming s^* and t^* are such that $\nabla_{\mathbf{q}}\phi_1^T\{\bar{\mathbf{q}}(s^*)\}h_1(s^*,t^*) = 0$ and $\nabla_{\theta_1}\phi_2^T\{\bar{\theta}_1(t^*)\}h_2(s^*,t^*) = 0$, or equivalently

$$\nabla_{\mathbf{q}}\phi_1^T\{\bar{\mathbf{q}}(s^*)\}\bar{s}(\bar{\mathbf{x}}(s^*,t^*)) = \nabla_{\mathbf{q}}\phi_1^T\{\bar{\mathbf{q}}(s^*)\}s^*$$
$$\nabla_{\theta_1}\phi_2^T\{\bar{\theta}_1(t^*)\}\bar{t}(\bar{\mathbf{x}}(s^*,t^*)) = \nabla_{\theta_1}\phi_2^T\{\bar{\theta}_1(t^*)\}t^*$$

By assumption 1, part (b), $\mathbf{q}^* = \bar{\mathbf{q}}(s^*)$ is the unique solution to (25a) and $\theta_1^* = \bar{\theta}_1(t^*)$ is the unique solution to (25b), i.e., $\nabla_{\mathbf{q}}\phi_1^T\{\bar{\mathbf{q}}(s^*)\}s^* = 0$, $\nabla_{\theta_1}\phi_2^T\{\bar{\theta}_1(t^*)\}t^* = 0$. Taking into account of the expression of $\nabla_{\mathbf{x}}K(\mathbf{x})$ given in (22), thus $\nabla_{\mathbf{x}}K(\mathbf{x})|_{\mathbf{x}=\bar{\mathbf{x}}(s^*,t^*)} = 0$. Then, from Proposition 1, s^* and t^* are roots of $h_1(s,t)$ and $h_2(s,t)$. The proof of Proposition 2 is now complete.

∎

C. The terms $\lambda_n \xi_1^n$, $\lambda_n \xi_2^n$, $\lambda_n r_1^n$ and $\lambda_n r_2^n$ tend to 0 with probability 1 as $n \to \infty$.

For the discrete time dynamical system (16) to be approximated by the ODE (20), we must show that $\lambda_n \xi_1^n$, $\lambda_n \xi_2^n$, $\lambda_n r_1^n$ and $\lambda_n r_2^n$ asymptotically tend to 0 with probability 1.

Denoting $M_{1,n,k} \triangleq \sum_{l=n}^{k} \lambda_l \xi_{1,l}$ and $M_{2,n,k} \triangleq \sum_{l=n}^{k} \lambda_l \xi_{2,l}$, following the proof of Proposition 1 in [29], it can be shown that $M_{1,n,k}$ and $M_{2,n,k}$ are martingales that satisfy $\lim_{n\to\infty} \sup_{k\geq n} |M_{1,n,k}| = 0$ and $\lim_{n\to\infty} \sup_{k\geq n} |M_{2,n,k}| = 0$, with probability 1. In addition, $\lim_{n\to\infty} r_{1,n} = 0$ and $\lim_{n\to\infty} r_{2,n} = 0$ by Proposition 1 in [29]. Following the proof of Theorem 1 in [22], it can then be shown that $\lim_{n\to\infty} d(\mathbf{x}_i^n, \mathcal{E}) = 0$ with probability 1, which completes the proof of Theorem 1.

APPENDIX C
TDOA MEASUREMENT SETUP

A. TDOA measurement principle

Let us start by emphasizing that our TDOA measurement setup *does not* aim at reproducing the distributed EM algorithm, but is used to measure the TDOA between different pair of nodes so that the distributed EM algorithm can be evaluated over real measurements offline.

Even when synchronized with GPS, a time offset remains between the different USRP receive nodes. When instructed to start measuring at a given time T_0, each node i will in reality start measuring at time T_{0i} which differs slightly from time T_0. This time offset between nodes results in a TDOA error that can be as large as 60 m. We now introduce a relaying architecture that cancels out this remaining time offset, provided that the clock skew is close to zero (which is the case in practice when using GPS-disciplined local oscillators). Let us consider the signal $x(t)$ sent by the transmitter. If we omit the effects of fading and noise for readability, the signal at the i-th node is given by $r_i(t) = x(t - \tau_{i1})$ where $\tau_{i1} = d_i/c_0$ is the propagation delay between the transmitter and node i (c_0 is the speed of light). The relay will start sampling the message at time T_{0i} (which might differ slightly for different relays), resulting in the sampled message $r_i[k] = x(T_{0i} + kT_s - \tau_{i1})$. Each relay node i will then forward its received message to a central receiver after a certain time delay T_{Di}, where a different time slot is allocated to each relay as to avoid collisions. The transmitted message from each relay is then given by

$$t_i(t) = \sum_{l=-\infty}^{\infty} x(T_{0i} + lT_s - \tau_{i1}) \cdot u(t - lT_s - T_{0i} - T_{Di})$$

where T_{Di} is the retransmission delay of the i-th node, and $u(t)$ is the pulse shaping filter of the node. The central receiver will start sampling the message from relay i at time $T_{0R} + T_{Di}$,

where T_{0R} is the central receiver's estimate of T_0. The sampled received message at the final receiver can be written as

$$r_R^{(i)}[n] = \sum_{l=-\infty}^{\infty} x(T_{0i} + lT_s - \tau_{i1}) \cdot g(T_{0R} + T_{Di} + nT_s - lT_s - T_{0i} - T_{Di} - \tau_{i2})$$

where τ_{i2} is the propagation delay between the i-th relay and the final receiver, and $g(t) = u(t) * u'(t)$ with $u'(t)$ being the pulse shaping filter at the receiver. If the pulse shaping filters are chosen appropriately and inter-symbol interference is canceled, the previous equation can be simplified to

$$r_R^{(i)}[n] = \sum_{l=-\infty}^{\infty} x(T_{0i} + lT_s - \tau_{i1}) \cdot \delta(T_{0R} + T_{Di} + (n - l)T_s - T_{0i} - T_{Di} - \tau_{i2}) \quad (28)$$

where $\delta(t)$ is the Dirac function. In (28), only one term in the sum is non-zero for a given n. In that case (28) simplifies to

$$r_R^{(i)}[n] = x(T_{0R} + nT_s - \tau_{i2} - \tau_{i1})$$

which is independent of the node measurement time T_{0i}. For different nodes (which forward the messages with different delays T_{Di}), the relayed messages at the central receiver will have identical offset T_{0R}. The proposed architecture is thus successfully able to cancel out differences in node measurement time offsets. The receiver then computes the ambiguity functions between the received messages $r_R^{(i)}[n]$ and $r_R^{(j)}[n]$ from nodes i and j. The index of the peak of the ambiguity function is then equal to $\tau_{i2} + \tau_{i1} - \tau_{j2} - \tau_{j1}$. If τ_{i2} and τ_{j2} are known, the receiver can recover the original TDOA $\tau_{i1} - \tau_{j1}$. The receiver is then able to compute the TDOA (expressed in distance) with respect to node 1 as follows:

$$\tilde{d}_{i1} = (\tau_{i1} - \tau_{11}) \cdot c_0$$

B. Experimental setup details

In our experimental setup, the relay nodes use USPR-N210 with WBX boards, which allows them to receive the signal from the transmitter on frequency f_1, and transmit the message after a delay T_{Di} to the central receiver over frequency f_2. The USRP drivers allow for very fine time control (down to one sample) of the received and transmitted samples. The central receiver consists of a USRP-N210 with a TVRX2 board, which is able to receive the signal from the transmitter on frequency f_1 and the signals from the relays on frequency f_2. All the USRPs in

TABLE II

Parameter	Value
RF source frequency f_1	795 MHz
RF source signal bandwidth	1 MHz
Relay/Rx sample rate	10 MHz
Relaying channel frequency f_2	755 MHz
Relay delay T_{Di}	$\{25, 50, 75\}$ ms
Recorded packet length	10 ms

our setup use GPSDO modules, which allows them to synchronize their internal clocks and local oscillators to the GPS UTC time. This is precise enough to have quasi-zero clock skew, but the clock offset between nodes can still be as high as 100 ns. In a off-line post-processing step, the central receiver oversamples the received messages by a factor of 10 and passes these signal through a low-pass filter, which allows to increase the resolution accuracy of our setup to 10 ns. Our setup was calibrated and tested extensively in a controlled environment with cables to avoid multipath and limited SNR problems. In those cases, our setup has an error below 10 ns. In an outdoor LOS setting, the TDOA error of our setup has a mean of 1 m and a standard deviation of 4 m. The RF source was a signal generator sending a random D-BPSK sequence. All the parameters of the setup are given in Table II. During the experiments, node S1 was chosen as the receiver node, while S0, S2 and S3 act as relay nodes.

In our TDOA measurement setup, one needs to know the propagation delay between the relay node and the central receiver to be able to estimate the propagation delay between the transmitter and the relay node. In our setup, this is achieved by creating a LOS link between the relay transmit antenna and the receiver. This is done by placing all the USRPs in Figure 7 on the same floor as the transmitter. The NLOS link for nodes S_2, S_3 and S_4 is created by using a 15 m cable between the USRP and the antenna that receives the signal over frequency f_1, which allows us to place this antenna on the upper floor corresponding to S_2 and S_4 in Figure 7, and behind the corner in the case of S_3. All the other antennas (for transmitting the relayed message in the case of S_1, S_3 and S_4, for receiving the relayed message in the case of S_2) are placed on the lower floor, and have a LOS to each other. The propagation delay between relay and receiver is then evaluated by measuring the distance between relays and receiver.

REFERENCES

[1] C. Knapp and G. C. Carter, "The generalized correlation method for estimation of time delay," *IEEE Trans. Acoust., Speech, Signal Process.*, vol. 24, no. 4, pp. 320–327, Aug 1976.

[2] G. Jacovitti and G. Scarano, "Discrete time techniques for time delay estimation," *IEEE Trans. Signal Process.*, vol. 41, no. 2, pp. 525–533, Feb 1993.

[3] Y. Chan and K. Ho, "A simple and efficient estimator for hyperbolic location," *IEEE Trans. Signal Process.*, vol. 42, no. 8, pp. 1905–1915, Aug 1994.

[4] T. Sathyan, A. Sinha, and T. Kirubarajan, "Passive geolocation and tracking of an unknown number of emitters," *IEEE Trans. Aerosp. Electron. Syst.*, vol. 42, no. 2, pp. 740–750, April 2006.

[5] K. Ho, X. Lu, and L. Kovavisaruch, "Source localization using TDOA and FDOA measurements in the presence of receiver location errors: Analysis and solution," *IEEE Trans. Signal Process.*, vol. 55, no. 2, pp. 684–696, Feb 2007.

[6] G. Mao, B. Fidan, and B. D. O. Anderson, "Wireless Sensor Network Localization Techniques," *Comput. Netw.*, vol. 51, no. 10, pp. 2529–2553, Jul. 2007. [Online]. Available: http://dx.doi.org/10.1016/j.comnet.2006.11.018

[7] G. Wang and H. Chen, "An Importance Sampling Method for TDOA-Based Source Localization," *IEEE Trans. Wireless Commun.*, vol. 10, no. 5, pp. 1560–1568, May 2011.

[8] K. H. Choi, W.-S. Ra, J. B. Park, and T. S. Yoon, "Compensated robust least-squares estimator for target localisation in sensor network using time difference of arrival measurements," *Signal Processing, IET*, vol. 7, no. 8, pp. 664–673, October 2013.

[9] L. Cong and W. Zhuang, "Non-line-of-sight error mitigation in TDOA mobile location," in *Global Telecommunications Conference, 2001. GLOBECOM '01. IEEE*, vol. 1, 2001, pp. 680 –684 vol.1.

[10] L. Yi, S. Gulam Razul, Z. Lin, and C.-M. See, "Individual AOA measurement detection algorithm for target tracking in mixed LOS/NLOS environments," in *IEEE Int. Conf. Acoustics, Speech, and Signal Processing*, 2013, pp. 3924–3928.

[11] B. Ananthasubramaniam and U. Madhow, "Cooperative localization using angle of arrival measurements in non-line-of-sight environments," in *Proc. ACM Int. Workshop on Mobile Entity Localization and Tracking in GPS-less Environments*, NY, USA, 2008, pp. 117–122.

[12] V. Ekambaram, K. Ramachandran, and R. Sengupta, "Collaborative High Accuracy Localization in Mobile Multipath Environments," *IEEE Trans. Veh. Technol.*, to be published, early Access.

[13] V. Algeier, B. Demissie, W. Koch, and R. Thom, "State space initiation for blind mobile terminal position tracking," *EURASIP Journal on Advances in Signal Processing, Special issue on Track Before Detect Algorithms*, vol. vol. 2008, no. 1, 2008.

[14] F. Yin, C. Fritsche, F. Gustafsson, and A. M. Zoubir, "TOA-based robust wireless geolocation and Cramr-Rao lower bound analysis in harsh LOS/NLOS environments," *IEEE Trans. Signal Process.*, vol. 61, no.9, pp. 2243–2255, 2013.

[15] ——, "EM- and JMAP-ML based joint estimation algorithms for robust wireless geolocation in mixed LOS/NLOS environments," *IEEE Trans. Signal Process.*, vol. 62, no.1, pp. 168–182, 2014.

[16] J. Li, J. Conan, and S. Pierre, "Mobile terminal location for MIMO communication systems," *IEEE Trans. Antennas Propag.*, vol. 55, no. 8, pp. 2417–2420, 2007.

[17] H. Miao, K. Yu, and M. Juntti, "Positioning for NLOS Propagation: Algorithm Derivations and Cramer–Rao Bounds," *IEEE Trans. Veh. Technol.*, vol. 56, no. 5, pp. 2568–2580, 2007.

[18] C. K. Seow and S. Y. Tan, "Non-line-of-sight localization in multipath environments," *IEEE Trans. Mobile Comput.*, vol. 7, no. 5, pp. 647–660, 2008.

[19] A. Dempster, N. Laird, and D. Rubin, "Maximum likelihood from incomplete data via the EM algorithm," *Journal of the Royal Statistical Society. Series B (Methodological)*, pp. 1–38, 1977.

[20] R. Nowak, "Distributed EM algorithms for density estimation and clustering in sensor networks," *IEEE Trans. Signal Process.*, vol. 51, no. 8, pp. 2245–2253, 2003.

[21] G. Morral, P. Bianchi, and J. Jakubowicz, "On-line gossip-based distributed expectation maximization algorithm," in *Statistical Signal Processing Workshop (SSP), 2012 IEEE*, 2012, pp. 305–308.

[22] O. Cappé and E. Moulines, "On-line expectation–maximization algorithm for latent data models," *Journal of the Royal Statistical Society: Series B (Statistical Methodology)*, vol. 71, no. 3, pp. 593–613, 2009.

[23] J. Fessler and A. Hero, "Space-alternating generalized expectation-maximization algorithm," *IEEE Trans. Signal Process.*, vol. 42, no. 10, pp. 2664–2677, 1994.

[24] M. Leng, W. P. Tay, and T. Q. S. Quek, "Cooperative and distributed localization for wireless sensor networks in multipath environments," in *IEEE Int. Conf. Acoustics, Speech, and Signal Processing*, Kyoto, Japan, Mar. 2012.

[25] J. Lang and D. Pai, "Bayesian estimation of distance and surface normal with a time-of-flight laser rangefinder," in *3-D Digital Imaging and Modeling, 1999. Proceedings. Second International Conference on*, 1999, pp. 109–117.

[26] V. Creuze, "Distance and orientation measurement of a flat surface by a single underwater acoustic transducer," in *Proc. European Signal Processing Conference*, 2011.

[27] Y. Chen and M. R. Gupta, "Em demystified: An expectation-maximization tutorial," Department of Electrical Engineering, University of Washington, Tech. Rep., 2010. [Online]. Available: https://www.ee.washington.edu/techsite/papers/documents/UWEETR-2010-0002.pdf

[28] P. J. Bickel and K. Doksum, *Mathematical Statistics: Basic Ideas and Selected Topics*, 2nd ed. Upper Saddle River, NJ: Prentice Hall, 2001, vol. 1.

[29] P. Bianchi and J. Jakubowicz, "Convergence of a Multi-Agent Projected Stochastic Gradient Algorithm for Non-Convex Optimization," *IEEE Trans. Autom. Control*, vol. 58, no. 2, pp. 391–405, 2013.

[30] S. Boyd, A. Ghosh, B. Prabhakar, and D. Shah, "Randomized gossip algorithms," *IEEE Trans. Inf. Theory*, vol. 52, no. 6, pp. 2508–2530, 2006.

[31] H.-J. Kim, J. up Kim, J.-H. Kim, H. Wang, and I.-S. Lee, "The Design Method and Performance Analysis of RF Subsampling Frontend for SDR/CR Receivers," *IEEE Trans. Ind. Electron.*, vol. 57, no. 5, pp. 1518–1525, May 2010.

[32] R. Schmidt, "Multiple emitter location and signal parameter estimation," *IEEE Trans. Antennas Propag.*, vol. 34, no. 3, pp. 276–280, Mar 1986.

[33] USRP products, http://www.ettus.com, 2013.